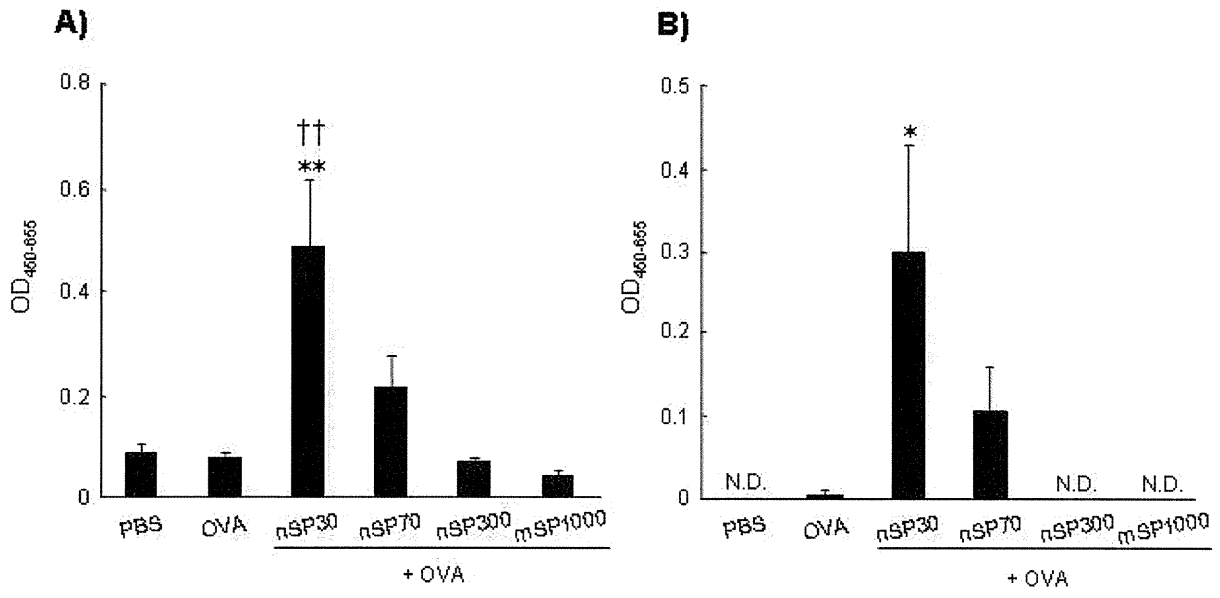

Figure 2 Plasma OVA-specific IgG and subclass IgG1 Ab response after intranasal exposure to OVA plus silica particles. BALB/c mice were intranasally exposed to PBS (vehicle control), OVA alone or OVA plus silica particles (250 μg/mouse) on days 0, 1, and 2. Plasma was collected on day 21 and analyzed by ELISA to detect the level of **(a)** OVA-specific IgG and **(b)** OVA-specific IgG1 Ab responses. Data represent mean absorbance at a wavelength of 450 nm (reference wavelength, 655 nm). N.D., not detected. Data are presented as mean ± SEM (n = 5 to 8); $^{*}P < 0.05$, $^{**}P < 0.01$ vs OVA alone; $^{\dagger\dagger}P < 0.01$ vs PBS).

(Figure 2). These results suggest that nanosilica particles can induce the production of antigen-specific Ab responses including antigen-specific Th2 allergic immune responses.

Antigen-specific cytokine responses of silica particles

To clarify the mechanism by which nSP30 elicited an immune response, we analyzed the profiles of cytokines released from splenocytes of OVA-exposed mice. The splenocytes were cultured in the presence of OVA *in vitro*, and the culture supernatants were assessed for Th2-type cytokines by using a multiplexed immunobeads assay. Splenocytes from mice exposed to OVA plus nSP30 exhibited higher levels of Th2-type cytokines (IL-4 and IL-5) than those induced with OVA alone (Figure 3). In contrast, there was hardly any difference in Th1-type cytokine (IFN-γ) production amongst all of the exposed mice (data not shown). In addition, nSP70, nSP300, and mSP1000 did not induce cytokine production (Figure 3). These results suggest that nSP30 nanosilica particle induces a Th2-type immune response in this experiment.

It is not clear why nanosilica particles such as nSP30 would induce Th2-polarized allergic immunity. Our results support previous reports showing that the immune-activating effect of nanomaterials increases with decreasing particle size [12,17]. The mechanisms behind the immune-activating effect of nanomaterials have not been fully elucidated. Nygaard et al [17] showed that the higher specific surface area of nanomaterials as compared to micro-sized particles allows more antigen to be adsorbed per particle. We consider that one possible mechanism by which allergic immune responses induced by nanosilica particles is that many antigen-captured nanomaterials might be taken up by professional antigen presenting cells, such as dendritic cells. Another possible mechanism is that the nanomaterials induce oxidative stress [18,19]. We have observed that nanosilica particles such as nSP30 are stronger inducers of oxidative stress than larger silica particles (unpublished data). Because there is accumulating evidence that oxidative stress plays a role in pro-inflammatory and immune-activating effects [20,21], dendritic cells might be activated more efficiently by nSP30 than by larger silica particles. Furthermore, we also observed that induction of oxidative stress by nanosilica particles is decreased by surface modification of nanosilica particles (unpublished data). Therefore, surface modification might be one approach to decrease allergic immune responses induced by nanosilica particles.

Conclusion

Here, we show that nanosilica particles have the potential to induce allergic immune responses after intranasal exposure. We consider that further studies of the relationship between the characteristics of nanomaterials

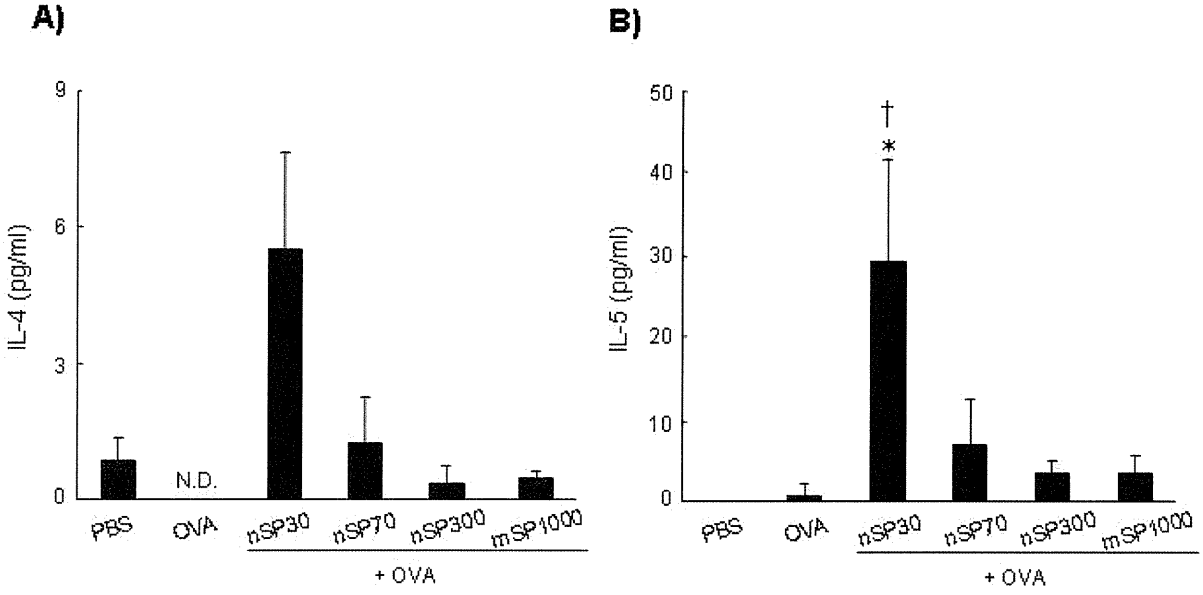

Figure 3 Cytokine responses induced after intranasal exposure to OVA plus silica particles. BALB/c mice were intranasally exposed to PBS (vehicle control), OVA alone or OVA plus silica particles (250 μg/mouse) on days 0, 1, and 2. On day 21, splenocytes from each group were prepared and cultured with 1 mg/mL OVA. Culture supernatants were harvested after 3 days of incubation, and the level of OVA-induced IL-4 (A) and IL-5 (B) produced and released into the culture supernatant was analyzed using the Bio-Plex Multiplex Cytokine Assay. Data are presented as mean ± SEM (n = 3; $^{*}P < 0.05$ vs OVA alone; $^{\dagger}P < 0.05$ vs PBS).

and allergic immune responses will facilitate the development of safe and effective nanomaterials.

Acknowledgements
This study was supported in part by Grants-in-Aid for Scientific Research from the Ministry of Education, Culture, Sports, Science and Technology of Japan, and from the Japan Society for the Promotion of Science. This study was also supported in part by Health Labor Sciences Research Grants from the Ministry of Health, Labor and Welfare of Japan; by Health Sciences Research Grants for Research on Publicly Essential Drugs and Medical Devices from the Japan Health Sciences Foundation; by a Global Environment Research Fund from Minister of the Environment; and by a the Knowledge Cluster Initiative; and by Food Safety Commission; and by The Nagai Foundation Tokyo; and by The Cosmetology Research Foundation; and by The Smoking Research Foundation.

Author details
[1]Department of Toxicology and Safety Science, Graduate School of Pharmaceutical Sciences, Osaka University, 1-6, Yamadaoka, Suita, Osaka 565-0871, Japan [2]Laboratory of Biopharmaceutical Research, National Institute of Biomedical Innovation, 7-6-8 Saito-asagi, Ibaraki, Osaka 567-0085, Japan [3]The Center for Advanced Medical Engineering and Informatics, Osaka University, 1-6, Yamadaoka, Suita, Osaka 565-0871, Japan [4]Department of Biomedical Innovation, Graduate school of Pharmaceutical Sciences, Osaka University, 7-6-8 Saito-asagi, Ibaraki, Osaka 567-0085, Japan

Authors' contributions
TY and YY designed the study; TY, MF, KY, KH, YM and HK performed experiments; TY, YY and MF collected and analysed data; TY and YY wrote the manuscript; HN, KN, YA, HK, ST, NI and TY gave technical support and conceptual advice. YT supervised the all of projects. All authors discussed the results and commented on the manuscript.

Competing interests
The authors declare that they have no competing interests.

Received: 7 October 2010 Accepted: 4 March 2011
Published: 4 March 2011

References

1. Fadeel B, Garcia-Bennett AE: **Better safe than sorry: Understanding the toxicological properties of inorganic nanoparticles manufactured for biomedical applications.** *Adv Drug Deliv Rev* 2010, **62**:362-374.
2. Barik TK, Sahu B, Swain V: **Nanosilica-from medicine to pest control.** *Parasitol Res* 2008, **103**:253-258.
3. Bharali DJ, Klejbor I, Stachowiak EK, Dutta P, Roy I, Kaur N, Bergey EJ, Prasad PN, Stachowiak MK: **Organically modified silica nanoparticles: a nonviral vector for in vivo gene delivery and expression in the brain.** *Proc Natl Acad Sci USA* 2005, **102**:11539-11544.
4. Bottini M, D'Annibale F, Magrini A, Cerignoli F, Arimura Y, Dawson MI, Bergamaschi E, Rosato N, Bergamaschi A, Mustelin T: **Quantum dot-doped silica nanoparticles as probes for targeting of T-lymphocytes.** *Int J Nanomedicine* 2007, **2**:227-233.
5. Kagan VE, Bayir H, Shvedova AA: **Nanomedicine and nanotoxicology: two sides of the same coin.** *Nanomedicine* 2005, **1**:313-316.
6. Nel A, Xia T, Madler L, Li N: **Toxic potential of materials at the nanolevel.** *Science* 2006, **311**:622-627.
7. Albrecht C, Schins RP, Hohr D, Becker A, Shi T, Knaapen AM, Borm PJ: **Inflammatory time course after quartz instillation: role of tumor necrosis factor-alpha and particle surface.** *Am J Respir Cell Mol Biol* 2004, **31**:292-301.
8. He X, Nie H, Wang K, Tan W, Wu X, Zhang P: **In vivo study of biodistribution and urinary excretion of surface-modified silica nanoparticles.** *Anal Chem* 2008, **80**:9597-9603.
9. Morishige T, Yoshioka Y, Inakura H, Tanabe A, Yao X, Narimatsu S, Monobe Y, Imazawa T, Tsunoda S, Tsutsumi Y, Mukai Y, Okada N, Nakagawa S: **The effect of surface modification of amorphous silica particles on NLRP3 inflammasome mediated IL-1beta production, ROS production and endosomal rupture.** *Biomaterials* 2010, **31**:6833-6842.
10. Morishige T, Yoshioka Y, Tanabe A, Yao X, Tsunoda S, Tsutsumi Y, Mukai Y, Okada N, Nakagawa S: **Titanium dioxide induces different levels of IL-1beta production dependent on its particle characteristics through**

caspase-1 activation mediated by reactive oxygen species and cathepsin B. *Biochem Biophys Res Commun* 2010, **392**:160-165.
11. Nishimori H, Kondoh M, Isoda K, Tsunoda S, Tsutsumi Y, Yagi K: **Silica nanoparticles as hepatotoxicants.** *Eur J Pharm Biopharm* 2009, **72**:496-501.
12. de Haar C, Hassing I, Bol M, Bleumink R, Pieters R: **Ultrafine but not fine particulate matter causes airway inflammation and allergic airway sensitization to co-administered antigen in mice.** *Clin Exp Allergy* 2006, **36**:1469-1479.
13. Nygaard UC, Hansen JS, Samuelsen M, Alberg T, Marioara CD, Lovik M: **Single-walled and multi-walled carbon nanotubes promote allergic immune responses in mice.** *Toxicol Sci* 2009, **109**:113-123.
14. Bonner JC: **Nanoparticles as a potential cause of pleural and interstitial lung disease.** *Proc Am Thorac Soc* 2010, **7**:138-141.
15. Finkelman FD, Hogan SP, Hershey GK, Rothenberg ME, Wills-Karp M: **Importance of cytokines in murine allergic airway disease and human asthma.** *J Immunol* 2010, **184**:1663-1674.
16. Yoshida T, Yoshioka Y, Fujimura M, Yamashita K, Higashisaka K, Nakanishi R, Morishita Y, Kayamuro H, Nabeshi H, Nagano K, Abe Y, Kamada H, Tsunoda S, Yoshikawa T, Itoh N, Tsutsumi Y: **Potential adjuvant effect of intranasal urban aerosols in mice through induction of dendritic cell maturation.** *Toxicol Lett* 2010, **199**:383-388.
17. Nygaard UC, Samuelsen M, Aase A, Lovik M: **The capacity of particles to increase allergic sensitization is predicted by particle number and surface area, not by particle mass.** *Toxicol Sci* 2004, **82**:515-524.
18. Brown DM, Wilson MR, MacNee W, Stone V, Donaldson K: **Size-dependent proinflammatory effects of ultrafine polystyrene particles: a role for surface area and oxidative stress in the enhanced activity of ultrafines.** *Toxicol Appl Pharmacol* 2001, **175**:191-199.
19. Shvedova AA, Kagan VE, Fadeel B: **Close encounters of the small kind: adverse effects of man-made materials interfacing with the nano-cosmos of biological systems.** *Annu Rev Pharmacol Toxicol* 2010, **50**:63-88.
20. Swindle EJ, Metcalfe DD: **The role of reactive oxygen species and nitric oxide in mast cell-dependent inflammatory processes.** *Immunol Rev* 2007, **217**:186-205.
21. Martinon F: **Signaling by ROS drives inflammasome activation.** *Eur J Immunol* 2010, **40**:616-619.

doi:10.1186/1556-276X-6-195
Cite this article as: Yoshida *et al.*: Promotion of allergic immune responses by intranasally-administrated nanosilica particles in mice. *Nanoscale Research Letters* 2011 **6**:195.

Department of Toxicology and Safety Science[1], Graduate School of Pharmaceutical Sciences, Osaka University; Laboratory of Biopharmaceutical Research[2], National Institute of Biomedical Innovation; The Center for Advanced Medical Engineering and Informatics[3], Osaka University, Osaka, Japan

Size-dependent immune-modulating effect of amorphous nanosilica particles

T. HIRAI[1,2], T. YOSHIKAWA[1,2], H. NABESHI[1,2], T. YOSHIDA[1,2], S. TOCHIGI[1,2], M. UJI[1,2], K. ICHIHASHI[1,2], T. AKASE[1,2], T. YAMASHITA[1,2], K. YAMASHITA[1,2], K. NAGANO[2], Y. ABE[2], H. KAMADA[2,3], S. TSUNODA[1,2,3], Y. YOSHIOKA[2,3], N. ITOH[1], Y. TSUTSUMI[1,2,3]

Received March 4, 2011, accepted April 8, 2011

Tomoaki Yoshikawa, Ph.D and Yasuo Tsutsumi, Ph.D, Department of Toxicology and Safety Science, Graduate School of Pharmaceutical Sciences, Osaka University 1-6 Yamadaoka, Suita, Osaka 565-0871, Japan
tomoaki@phs.osaka-u.ac.jp; ytsutsumi@phs.osaka-u.ac.jp

Pharmazie 66: 727–728 (2011)
doi: 10.1691/ph.2011.1529

The immune-modulating effect following intradermal injection of various-sized amorphous silica particles was analyzed in terms of induction of ovalbumin-specific CD8$^+$ T cells *in vivo*. IFN-γ ELISPOT assays revealed that only nanosilica particles with a diameter of less than 100 nm significantly enhanced CD8$^+$ T cell responses against ovalbumin. These results indicate that the size of nanomaterials is a critical determinant in terms of their safe use.

Recently, practical uses of nanomaterials (NMs) have rapidly spread to a wide variety of fields, such as cosmetics, foods, and medicines (Bowman et al. 2010; Liu and Gu 2009; Salata 2004). However, potential harmful effects of NMs on humans are raising concerns with regard to their safety, because NMs may possess novel properties different from micro-sized materials (Nel et al. 2006). Despite intensive research, the relationship between the biological response and physicochemical properties of NMs is not well understood. Specifically, it is important to clarify the relationship between particle-size and cellular distribution/associated biological effects, thereby facilitating a more accurate risk assessment of NMs.

Currently, amorphous nanosilica particles (nSPs) are among the most widely used NMs in a variety of different applications (Napierska et al. 2010). Here, we evaluated the relationship between the *in vivo* distributions of nSPs with their biological effect. Recently, we revealed that the nSPs with a diameter of 70 nm (nSP70) can penetrate the skin barrier and reach various tissues such as the lymph node, liver, and brain (Nabeshi et al. 2011). In a separate study, we also revealed that amorphous silica particles have size-dependent toxicity to murine Langerhans cell line XS52 (Nabeshi et al. 2010). Both the lymph nodes and Langerhans cells play a critical role in the immune response. Here, we wanted to clarify whether applications of nSPs induce an immune-modulating effect. Therefore, we investigated the induction of CD8$^+$ T cells in response to an exogenous antigen in the presence/absence of nSPs.

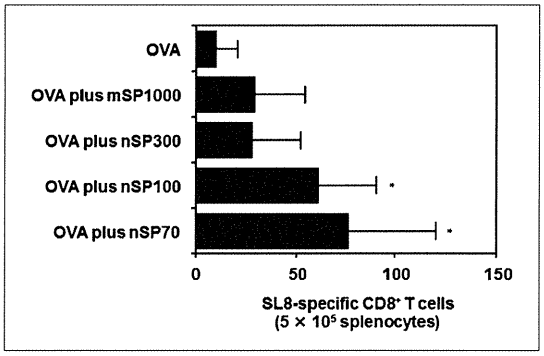

Fig.: Analysis of SL8 specific CD8$^+$ T cell response *in vivo*. C57BL/6 mice were intradermally immunized with OVA alone or OVA plus various sized silica particles. Six days after the immunization, splenocytes from each group were cultured with 5 μg/ml $OVA_{257-264}$ (SL8) peptide. The levels of SL8-specific CD8$^+$ T cells were examined using an IFN-γ ELISPOT assay. Data are presented as means ± SD of 3–4 animals per group. * $P < 0.05$ vs. OVA alone group.

Female C57BL/6 mice were intradermally immunized with ovalbumin (OVA) alone or OVA plus various sized silica particles. Six days after the immunization, splenocytes from each group were cultured with $OVA_{257-264}$ peptide (SL8), which corresponds to an immunodominant H-2K^b-restricted CD8$^+$ T cell-epitope of OVA. The levels of SL8-specific CD8$^+$ T cells were then examined using an IFN-γ ELISPOT assay. Our results show that induction of SL8-specific CD8$^+$ T cells was not enhanced in the submicron-sized silica particle immunized group. However, significant induction of SL8-specific CD8$^+$ T cells was observed in the group of mice immunized with OVA plus nSPs of diameter below 100 nm (Fig.). Moreover, the corresponding level of induction increased as the diameter of nSPs was reduced. Thus, nSPs can affect immune response against exogenous antigen.

Our results suggest that the intradermal injection of nSPs can affect CD8$^+$ T cell responses against exogenous antigen. Further studies are required to analyze the immune-modulating effect of nSPs using topical applications of nSPs, which is a more likely mode of exposure to NMs. We believed that a robust quantitative analysis of the results of exposure to nSPs will provide critical information to ensure the safety of nSPs. This study indicates that the sizes of NMs as well as the target cell type are critical determinants for the design of safer NMs. We believe that our study will provide useful information for developing safer NMs in the future.

Experimental

1. Silica particles

Amorphous silica particles with a diameter of 1000, 300, 100, 70 nm (designated mSP1000, nSP300, nSP100, nSP70, respectively; Micromod Partikeltechnologie GmbH, Rostock, Germany) were used in this study. The silica particles were suspended in phosphate-buffered saline (PBS; pH7.4). The suspensions of silica particles were sonicated for 5 min and then vortexed for 1 min immediately prior to use.

2. Evaluation of $OVA_{257-264}$ (SL8) -specific T cell responses in vivo

Female C57BL/6 mice (H-2K^b) were purchased from Japan SLC (Shizuoka, Japan) and used at 10 weeks of age. All of the animal experimental procedures were performed in accordance with the institutional ethical guidelines for animal experiments of Osaka University and National Institute of Biomedical Innovation. Mice were intradermally injected with either a mixture of 625 μg silicia particles and 100 μg OVA (Sigma Chemical Co., St.

Louis, MO) in the 50 μl PBS, or 100 μg OVA (50 μl/mouse) in the 50 μl PBS. Six days after immunization, splenocytes were prepared from these mice. The splenocytes were cultured *in vitro* (5×10^5 cells) and stimulated with $OVA_{257-264}$ peptide (SL8) (5 μg/ml), which corresponds to an immunodominant H-$2K^b$-restricted $CD8^+$ T cell-epitope of OVA (MBL, Nagoya, Japan). Cells were incubated for 24 h and the number of SL8 specific $CD8^+$ T cell was determined using an IFN-γ ELISPOT assay kit (BD Biosciences, San Diego, CA) according to manufacturer's protocol.

3. *Statistical analysis*

All data are reported as the mean ± SD. The significance of variation among different groups was determined by one-way ANOVA. Differences between the experimental group and control group were determined by Williams' test. $P < 0.05$ was considered significant.

Acknowledgement: This study was supported in part by Grants-in-Aid for Scientific Research from the Ministry of Education, Culture, Sports, Science and Technology of Japan (MEXT), and from the Japan Society for the Promotion of Science (JSPS); and by a the Knowledge Cluster Initiative (MEXT); by Health Labour Sciences Research Grants from the Ministry of Health, Labor and Welfare of Japan (MHLW); by a Global Environment Research Fund from Minister of the Environment; by Food Safety Commission (Cabinet Office); by The Cosmetology Research Foundation; by The Smoking Research Foundation; by The Takeda Science Foundation.

References

Bowman D M, van Calster G, Friedrichs S (2010) Nanomaterials and regulation of cosmetics. Nat Nanotechnol 5: 92.

Liu D, Gu N (2009) Nanomaterials for fresh-keeping and sterilization in food preservation. Recent Pat Food Nutr Agric 1: 149–154.

Nabeshi H, Yoshikawa T, Matsuyama K, Nakazato Y, Arimori A, Isobe M, Tochigi S, Kondoh S, Hirai T, Akase T, Yamashita T, Yamashita K, Yoshida T, Nagano K, Abe Y, Yoshioka Y, Kamada H, Imazawa T, Itoh N, Tsunoda S, and Tsutsumi Y (2010) Size-dependent cytotoxic effects of amorphous silica nanoparticles on Langerhans cells. Pharmazie 65: 199–201.

Nabeshi H, Yoshikawa T, Matsuyama K, Nakazato Y, Matsuo K, Arimori A, Isobe M, Tochigi S, Kondoh S, Hirai T, Akase T, Yamashita T, Yamashita K, Yoshida T, Nagano K, Abe Y, Yoshioka Y, Kamada H, Imazawa T, Itoh N, Nakagawa S, Mayumi T, Tsunoda S, Tsutsumi Y (2011) Systemic distribution, nuclear entry and cytotoxicity of amorphous nanosilica following topical application. Biomaterials 32: 2713–2724.

Napierska D, Thomassen L C, Lison D, Martens JA, Hoet PH (2010) The nanosilica hazard: another variable entity. Part Fibre Toxicol 7: 39.

Nel A, Xia T, Madler L, Li N (2006) Toxic potential of materials at the nanolevel. Science 311: 622–627.

Salata O (2004) Applications of nanoparticles in biology and medicine. J Nanobiotechnology 2: 3.

Nabeshi et al. Nanoscale Research Letters 2011, 6:464
http://www.nanoscalereslett.com/content/6/1/464

Nanoscale Research Letters
a SpringerOpen Journal

NANO EXPRESS Open Access

Effect of amorphous silica nanoparticles on *in vitro* RANKL-induced osteoclast differentiation in murine macrophages

Hiromi Nabeshi[1,2], Tomoaki Yoshikawa[1,2*], Takanori Akase[1,2], Tokuyuki Yoshida[1,2], Saeko Tochigi[1,2], Toshiro Hirai[1,2], Miyuki Uji[1,2], Ko-ichi Ichihashi[1,2], Takuya Yamashita[1,2], Kazuma Higashisaka[1,2], Yuki Morishita[1,2], Kazuya Nagano[2], Yasuhiro Abe[2], Haruhiko Kamada[2,3], Shin-ichi Tsunoda[2,3,4], Norio Itoh[1,2], Yasuo Yoshioka[2,3] and Yasuo Tsutsumi[1,2,3*]

Abstract

Amorphous silica nanoparticles (nSP) have been used as a polishing agent and/or as a remineralization promoter for teeth in the oral care field. The present study investigates the effects of nSP on osteoclast differentiation and the relationship between particle size and these effects. Our results revealed that nSP exerted higher cytotoxicity in macrophage cells compared with submicron-sized silica particles. However, tartrate-resistant acid phosphatase (TRAP) activity and the number of osteoclast cells (TRAP-positive multinucleated cells) were not changed by nSP treatment in the presence of receptor activator of nuclear factor κB ligand (RANKL) at doses that did not induce cytotoxicity by silica particles. These results indicated that nSP did not cause differentiation of osteoclasts. Collectively, the results suggested that nanosilica exerts no effect on RANKL-induced osteoclast differentiation of RAW264.7 cells, although a detailed mechanistic examination of the nSP70-mediated cytotoxic effect is needed.

Keywords: silicon dioxide, nanoparticle, osteoclast differentiation

Introduction

Recently, amorphous silica nanoparticles (nSP) with a controlled particle size below 100 nm have been a focus of investigations in various fields of industry. nSP have been used in a number of different industrial applications such as medicine, cosmetics and foods. In addition, the usability of nSP has been demonstrated in the oral care field, e.g. as a polishing agent and/or as a remineralization promoter for teeth [1,2]. It has been reported that about 20% of toothpastes contain nSP. Because nSP have already become commonly used materials, it is difficult to imagine our daily life without them. Furthermore, given the recent use of smaller-sized and/or well-dispersed silica particles in various fields, it is expected that the use of these particles will increase in the future. On the other hand, there have been many reports that nSP exert biological effects that are not induced by conventional silica particles [3,4], although the reasons for the effects of particle size on biological responses were unclear. There are growing concerns about the safety of nSP [5]. However, current risk analyses do not yet focus sufficiently on the particle sizes. Accordingly, there is a compelling need to clarify the biological and cellular responses induced by different particle sizes. To ensure the safe production and use of nSP, it is very important to collect safety information on them via properly designed studies, taking into consideration exposure levels and cellular responses.

Our group carried out a previous study of the safety of nSP and revealed that surface unmodified nSP could pass though the skin barrier, migrate into the bloodstream and circulate throughout the entire body [6]. This suggests that nSP may be absorbed through the oral mucosa easily when nSP, including oral care products, are used. Furthermore, it is possible that nSP circulating in the blood can reach the alveolar bone, which is presented in the submucosal layer, as well as various cells such as macrophages and osteoblasts. In particular, macrophages are known as multifunctional cells, as they

* Correspondence: tomoaki@phs.osaka-u.ac.jp; ytsutsumi@phs.osaka-u.ac.jp
[1]Laboratory of Toxicology and Safety Science, Graduate School of Pharmaceutical Sciences, Osaka University, 1-6 Yamadaoka, Suita, Osaka 565-0871, Japan
Full list of author information is available at the end of the article

can function not only as immunocompetent cells, but also as pre-osteoclasts [7]. Osteoclasts that resorb bone play an important role in bone remodelling. Osteoclastogenesis involves complex pathways with intricate relationships between multiple signalling molecules. In particular, receptor activator of nuclear factor κB ligand (RANKL) is known to be a key molecule that initiates osteoclast formation [8]. In addition, reactive oxygen species (ROS) and pro-inflammatory cytokines such as interleukin (IL)-1, IL-6, IL-8 and tumour necrosis factor alpha are potent stimulators of osteoclast formation and activity [9-11]. Our studies revealed that nSP induced high ROS and pro-inflammatory cytokine production, and these cellular responses may induce excess osteoclast differentiation. Acceleration of osteoclast differentiation, that is excess bone resorption, accelerates the onset of osteoporosis, arthritis and periodontal disease [12-14]. Therefore, we consider that it is necessary to estimate nSP-induced effects on osteoclast differentiation. Furthermore, because we indicated previously that nSP induced different cellular responses from submicron-sized silica particles, such as those described above, it was of interest to analyse the effects of particle size on osteoclast differentiation. Here, we investigate nSP-induced effects on osteoclast differentiation and the relationship between particle size and these effects.

Experimental procedures

Silica particles

Suspensions of amorphous silica particles (Micromod Partikeltechnologie GmbH, Warnemuende, Germany) (25 and 50 mg/ml) were used in this study; particle size diameters were 70, 300 and 1,000 nm (designated as nSP70, nSP300 and mSP1000, respectively). Silica particle suspensions were stored at room temperature. The suspensions were sonicated for 5 min and then vortexed for 1 min immediately prior to use.

Cell culture

The mouse macrophage cell line RAW264.7 was obtained from the American Type Culture Collection (ATCC, Manassas, VA, USA). RAW264.7 cells were cultured in Dulbecco's Modified Eagle Medium supplemented with 10% heat-inactivated fetal calf serum (FCS), 1% antibiotic-antimycotic mix stock solution (Invitrogen Corporation, Carlsbad, CA, USA). All cultures were incubated at 37°C in a humidified atmosphere with 5% CO_2.

Cytotoxicity test

The cytotoxicity of silica particle-treated RAW264.7 cells and untreated cells was assessed using a WST-8 assay. Cells, 1.5×10^3, were cultured with varying concentrations of silica particles diluted with medium for 5 days at 37°C and 10 μl of Cell Count Reagent SF (Nacalai Tesque, Inc., Kyoto, Japan) was then added into each well. After 1 h, absorbance was measured at 450 nm (reference, 650 nm) using a microplate reader (Mithras LB940; BERTHOLD TECHNOLOGIES GmbH & Co. KG, Bald Wildbad, Germany).

TRAP staining and activity assay

Osteoclast differentiation of silica particle-treated RAW264.7 cells was assessed by tartrate-resistant acid phosphatase (TRAP) staining and activity. RAW264.7 cells were suspended in phenol red-free α-MEM containing 10% heat-inactivated FCS, 1% antibiotic-antimycotic mix stock solution. Cells numbering 2×10^4 per well were cultured in 48-well plates with 10 μg/ml of silica particles and RANKL (30 ng/ml) diluted with phenol red-free medium for 5 days. TRAP staining was carried out using a TRAP/alkaline phosphatase (ALP) stain kit (Wako Pure Chemicals Industries Ltd., Osaka, Japan) according to the protocol provided in the kit. Images of TRAP-positive multinucleated cells (number of nuclei > 3) were captured with a microscope. To measure TRAP activity, cells were fixed with 10% formalin for 10 min and 95% ethanol for 1 min, and then 100 μl of citrate buffer (50 mM, pH 4.6) containing 10 mM sodium tartrate and 5 mM p-nitrophenylphosphate (Sigma-Aldrich Corporation, St. Louis, MO, USA) was added to the wells containing fixed cells in the 48-well plates. After incubation for 1 h, enzyme reaction mixtures in the wells were transferred to new plates containing an equal volume of 0.1 N NaOH. Absorbance was measured at 410 nm using a microplate reader (Mithras LB940; BERTHOLD TECHNOLOGIES GmbH & Co. KG, Bald Wildbad, Germany). Each experiment was performed in triplicate.

Statistical analysis

All data are reported as the mean ± SD. The significance of variation among different groups was determined by one-way ANOVA. Differences between the experimental and control groups were determined using the Bonferroni test. $P < 0.05$ was considered significant.

Results and discussion

This study evaluated the effects of amorphous silica particles on osteoclast differentiation of macrophage cells, using silica particles of 70 (nSP70), 300 (nSP300) and 1,000 nm (mSP1000) in diameter. We previously confirmed that these silica particles were spherical, and the primary particle sizes were approximately uniform [6]. In addition, none of the silica particles used in this study were modified with any functional groups, and their surfaces were nonporous. The mean particle size in PBS suggested that the silica particles used in this

study remained as stable well-dispersed particles in solution, i.e. they did not aggregate [6].

To evaluate the cytotoxicity induced by silica particle treatment of the mouse macrophage cell line RAW264.7 cells, a WST-8 cell proliferation assay was carried out. The results showed that 30 μg/ml of nSP300 and mSP1000 treatment for 5 days did not induce cytotoxicity in RAW264.7 cells. In contrast, nSP70 treatment induced higher cytotoxicity (about 40% viability of non-treated cells) at 30 μg/ml, although 10 μg/ml of nSP70 treatment produced only marginal cytotoxicity (Figure 1). These results indicated that decreasing the silica particle size to below 100 nm increased the cytotoxicity significantly. We have confirmed that the number of silica particles ingested by cells increases as the particle size decreases, and only nSP70 invaded into the nuclei of dendritic cells which, along with macrophages, have a phagocytic capacity [15]. We also found that only nSP70 invaded into the nucleus, in other words the intracellular localization of nSP70 differed from that of nSP300 and mSP1000 [15]. From these results, it was suspected that differences in the number of ingested silica particles and/or in their intracellular localization were significant factors in their observed cytotoxicity in RAW264.7 cells. Results of this experiment confirmed that not all silica particles induced cytotoxicity at 10 μg/ml in RAW264.7 cells, and therefore subsequent studies were carried out at 10 μg/ml silica particle treatment.

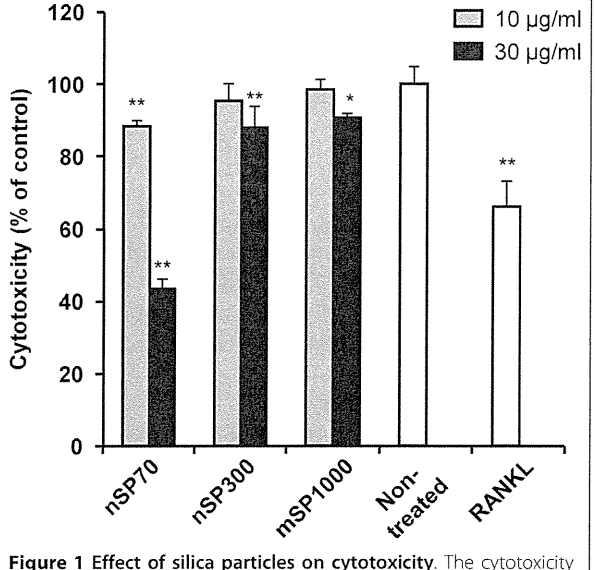

Figure 1 Effect of silica particles on cytotoxicity. The cytotoxicity of RAW264.7 cells after incubation with nSP70, nSP300 or mSP1000 for 5 days was evaluated using the WST-8 assay. The percentage increase in cytotoxicity was calculated relative to the negative control. Data are expressed as the mean ± SD (n = 3). *P < 0.05, **P < 0.01 vs non-treated.

In order to investigate the effects of nanosilica on osteoclast differentiation in RAW264.7 cells, TRAP activity, which is a known indicator of osteoclast differentiation, was measured. TRAP activity levels of RANKL (which is a key molecule in osteoclast differentiation)-treated RAW264.7 cells were significantly increased compared to non-treated RAW264.7 cells (Figure 2). On the other hand, TRAP activity levels of RAW264.7 cells treated with RANKL and silica particles were almost equal to those of cells treated with RANKL alone. An analysis comparing TRAP activities between nSP70, nSP300 and mSP1000 did not reveal significant size-dependent changes (Figure 2). Furthermore, the number of TRAP-positive multinucleated cells were tallied as a measure of osteoclast differentiation by RANKL and silica particle treatment. As a result of TRAP staining, RAW264.7 cells treated by RANKL alone or by RANKL with silica particles were almost all TRAP positive (Figure 3). The number of TRAP-positive multinucleated cells indicated no significant differences following each silica particle treatment, although nSP70-treated RAW264.7 cells tended to have an increased number of TRAP-positive multinucleated cells compared to cells treated with RANKL alone (Figure 4). These results suggested that none of the silica particle sizes used in this study induced effects on osteoclast differentiation of RAW264.7 cells at the doses given.

In the dentistry field, it is well-known that wear particles from materials used in implants can induce bone destruction, and this can become a significant

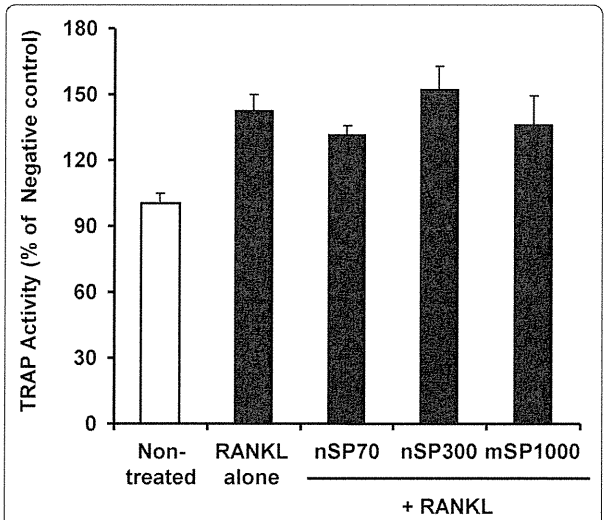

Figure 2 Effect of silica particles on the RANKL-induced TRAP activity in RAW264.7 cells. RAW264.7 cells were incubated with 10 μg/ml silica particles and 30 ng/ml RANKL for 5 days. TRAP activity was calculated relative to the negative controls (medium without RANKL). Data are expressed as the mean ± SD (n = 3).

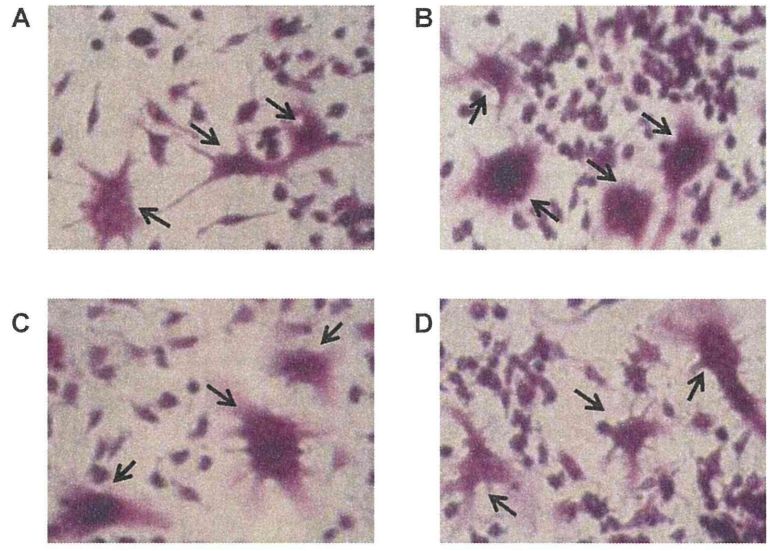

Figure 3 Effect of silica particles on the RANKL-induced osteoclast differentiation in RAW264.7 cells (TRAP staining). RAW264.7 cells were incubated with 10 μg/ml silica particles and 30 ng/ml RANKL for 5 days. Osteoclast genesis was confirmed by TRAP staining. (**A**) RANKL alone (30 ng/ml), (**B**) nSP70 10 μg/ml with RANKL 30 ng/ml, (**C**) nSP300 10 μg/ml with RANKL 30 ng/ml, (**D**) mSP1000 10 μg/ml with RANKL 30 ng/ml. Arrows show osteoclast cells (TRAP-positive multinucleate cells (> 3 nuclei)). Magnifications of all photographs are ×400.

therapeutic problem in the treatments requiring implants and/or artificial bone. Some reports have suggested that micro-sized particles (about 4-9 μm in diameter) increased the expression of RANKL and/or osteoclast differentiation-related genes in bone marrow cells [16,17]. These reports suggested that micro-sized particles above 4 μm accelerated the osteoclast differentiation. On the other hand, in the case of nano- and subnano-sized particles, it has been reported that particles did not affect osteoclast differentiation or the expression of inflammatory cytokines and osteoclast differentiation-regulated genes [18]. Our earlier results and the present report suggest that acceleration effects of particles on osteoclast differentiation slowed as the particles got smaller, until they reached nanosize. In other words, the particle size is an important characteristic in the ability of nanoparticles to induce osteoclast differentiation. The mechanism by which cells take up particles differs according to particle sizes [19]. The larger particles (from several micrometers to several dozen micrometers) and the smaller particles (from several dozen to several hundred nanometers) are believed to be taken up by macrophage cells via phagocytosis and macropinocytosis, respectively [19]. Therefore, these differences of particle uptake pathway may be one of the factors producing the observed effect of particle size on osteoclast differentiation.

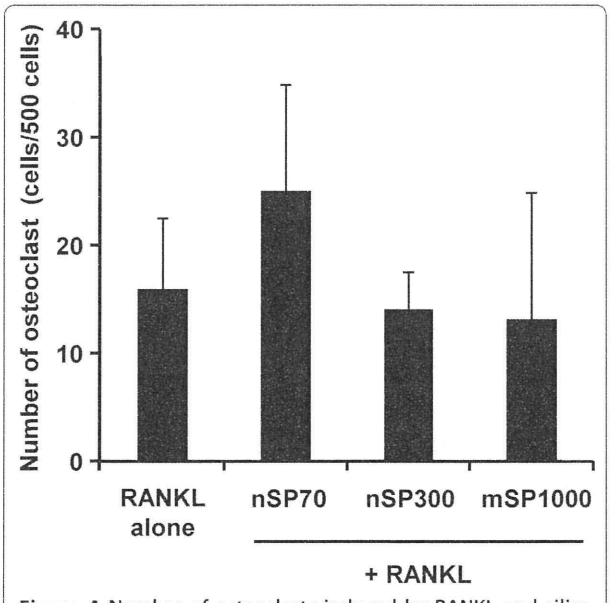

Figure 4 Number of osteoclasts induced by RANKL and silica particles in RAW264.7. RAW264.7 cells were incubated with 10 μg/ml silica particles and 30 ng/ml RANKL for 5 days. The number of TRAP-positive multinucleate cells (> 3 nuclei) were counted as osteoclasts in three different areas. Data are expressed as the mean ± SD (n = 3).

Collectively, the results presented here indicated that nanosilica has no effect on osteoclast differentiation. They also support the safety of nanosilicas that are used in the production of highly functional materials for oral care fields [1,20]. We believe that applications of nanosilica will extend to these new fields in the near future following further careful safety study.

Acknowledgements
This study was supported in part by Grants-in-Aid for Scientific Research from the Ministry of Education, Culture, Sports, Science and Technology of Japan (MEXT), and from the Japan Society for the Promotion of Science (JSPS); and by a the Knowledge Cluster Initiative (MEXT); by Health Labour Sciences Research Grants from the Ministry of Health, Labour and Welfare of Japan (MHLW); by a Global Environment Research Fund from Minister of the Environment; by Food Safety Commission (Cabinet Office); by The Cosmetology Research Foundation; by The Smoking Research Foundation; and by The Takeda Science Foundation.

Author details
[1]Laboratory of Toxicology and Safety Science, Graduate School of Pharmaceutical Sciences, Osaka University, 1-6 Yamadaoka, Suita, Osaka 565-0871, Japan [2]Laboratory of Biopharmaceutical Research (Pharmaceutical Proteomics), National Institute of Biomedical Innovation, 7-6-8 Saito-Asagi, Ibaraki, Osaka 567-0085, Japan [3]The Center for Advanced Medical Engineering and Informatics, Osaka University, 1-6 Yamadaoka, Suita, Osaka 565-0871, Japan [4]Laboratory of Biomedical Innovation, Graduate School of Pharmaceutical Sciences, Osaka University, 7-6-8 Saito-Asagi, Ibaraki, Osaka, 567-0085, Japan

Authors' contributions
HN and TY designed the study. HN, TA, TY, ST, TH, MU, KI, TY, KH and YM performed experiments. HN and TY collected and analysed data. HN and TY wrote the manuscript. KN, YA, HK, ST, NI and YY gave technical support and conceptual advice. YT supervised all of the projects. All authors discussed the results and commented on the manuscript.

Competing interests
The authors declare that they have no competing interests.

Received: 18 April 2011 Accepted: 22 July 2011 Published: 22 July 2011

References

1. Gaikwad RM, Sokolov I: **Silica nanoparticles to polish tooth surfaces for caries prevention.** *J Dent Res* 2008, **87**:980-983.
2. Liao WQ, Zang YL, Shao JZ: **Sporotrichosis presenting as pyoderma gangrenosum.** *Mycopathologia* 1991, **116**:165-168.
3. Napierska D, Thomassen LC, Lison D, Martens JA, Hoet PH: **The nanosilica hazard: another variable entity.** *Part Fibre Toxicol* 2010, **7**:39.
4. Yamashita K, Yoshioka Y, Higashisaka K, Mimura K, Morishita Y, Nozaki M, Yoshida T, Ogura T, Nabeshi H, Nagano K, Abe Y, Kamada H, Monobe Y, Imazawa T, Aoshima H, Shishido K, Kawai Y, Mayumi T, Tsunoda SI, Itoh N, Yoshikawa T, Yanagihara I, Saito S, Tsutsumi Y: **Nat Nanotechnol.** 2011.
5. Maynard AD, Aitken RJ, Butz T, Colvin V, Donaldson K, Oberdörster G, Philbert MA, Ryan J, Seaton A, Stone V, Tinkle SS, Tran L, Walker NJ, Warheit DB: **Safe handling of nanotechnology.** *Nature* 2006, **444**:267-269.
6. Nabeshi H, Yoshikawa T, Matsuyama K, Nakazato Y, Matsuo K, Arimori A, Isobe M, Tochigi S, Kondoh S, Hirai T, Akase T, Yamashita T, Yamashita K, Yoshida T, Nagano K, Abe Y, Yoshioka Y, Kamada H, Imazawa T, Itoh N, Nakagawa S, Mayumi T, Tsunoda S, Tsutsumi Y: **Systemic distribution, nuclear entry and cytotoxicity of amorphous nanosilica following topical application.** *Biomaterials* 2011, **32**:2713-2724.
7. Ash P, Loutit JF, Townsend KM: **Osteoclasts derived from haematopoietic stem cells.** *Nature* 1980, **283**:669-670.
8. Suda T, Takahashi N, Udagawa N, Jimi E, Gillespie MT, Martin TJ: **Modulation of osteoclast differentiation and function by new members of the tumor necrosis factor receptor and ligand families.** *Endocr Rev* 1999, **20**:345-357.
9. Dougall WC, Glaccum M, Charrier K, Rohrbach K, Brasel K, De Smedt T, Daro E, Smith J, Tometsko ME, Maliszewski CR, Armstrong A, Shen V, Bain S, Cosman D, Anderson D, Morrissey PJ, Peschon JJ, Schuh J: **RANK is essential for osteoclast and lymph node development.** *Genes Dev* 1999, **13**:2412-2424.
10. Wiktor-Jedrzejczak W, Bartocci A, Ferrante AW, Ahmed-Ansari A, Sell KW, Pollard JW, Stanley ER: **Total absence of colony-stimulating factor 1 in the macrophage-deficient osteopetrotic (op/op) mouse.** *Proc Natl Acad Sci USA* 1990, **87**:4828-4832.
11. Yoshida H, Hayashi S, Kunisada T, Ogawa M, Nishikawa S, Okamura H, Sudo T, Shultz LD: **The murine mutation osteopetrosis is in the coding region of the macrophage colony stimulating factor gene.** *Nature* 1990, **345**:442-444.
12. Takayanagi H: **Osteoimmunology: shared mechanisms and crosstalk between the immune and bone systems.** *Nat Rev Immunol* 2007, **7**:292-304.
13. Teitelbaum SL, Ross FP: **Genetic regulation of osteoclast development and function.** *Nat Rev Genet* 2003, **4**:638-649.
14. Theill LE, Boyle WJ, Penninger JM: **RANK-L and RANK: T cells, bone loss, and mammalian evolution.** *Annu Rev Immunol* 2002, **20**:795-823.
15. Nabeshi H, Yoshikawa T, Matsuyama K, Nakazato Y, Arimori A, Isobe M, Tochigi S, Kondoh S, Hirai T, Akase T, Yamashita T, Yamashita K, Yoshida T, Nagano K, Abe Y, Yoshioka Y, Kamada H, Imazawa T, Itoh N, Tsunoda S, Tsutsumi Y: **Size-dependent cytotoxic effects of amorphous silica nanoparticles on Langerhans cells.** *Pharmazie* 2010, **65**:199-201.
16. Clohisy JC, Frazier E, Hirayama T, Abu-Amer Y: **RANKL is an essential cytokine mediator of polymethylmethacrylate particle-induced osteoclastogenesis.** *J Orthop Res* 2003, **21**:202-212.
17. Pioletti DP, Kottelat A: **The influence of wear particles in the expression of osteoclastogenesis factors by osteoblasts.** *Biomaterials* 2004, **25**:5803-5808.
18. Tautzenberger A, Kreja L, Zeller A, Lorenz S, Schrezenmeier H, Mailänder V, Landfester K, Ignatius A: **Direct and indirect effects of functionalised fluorescence-labelled nanoparticles on human osteoclast formation and activity.** *Biomaterials* 2010, **32**:1706-1714.
19. Hillaireau H, Couvreur P: **Nanocarriers' entry into the cell: relevance to drug delivery.** *Cell Mol Life Sci* 2009, **66**:2873-2896.
20. Muller WE, Boreiko A, Wang X, Krasko A, Geurtsen W, Custodio MR, Winkler T, Lukic-Bilela L, Link T, Schroder HC: **Morphogenetic activity of silica and bio-silica on the expression of genes controlling biomineralization using SAOS-2 cells.** *Calcif Tissue Int* 2007, **81**:382-393.

doi:10.1186/1556-276X-6-464
Cite this article as: Nabeshi *et al.*: Effect of amorphous silica nanoparticles on *in vitro* RANKL-induced osteoclast differentiation in murine macrophages. *Nanoscale Research Letters* 2011 **6**:464.

Department of Toxicology and Safety Science[1], Graduate School of Pharmaceutical Sciences; The Center for Advanced Medical Engineering and Informatics[2], Osaka University, Osaka; Japan Synchrotron Radiation Research Institute[3], Hyogo, Japan

Detection of titanium dioxide particles on frozen tissue sections using synchrotron radiation X-ray fluorescence analysis

Y. MORISHITA[1,*], K. YAMASHITA[1,*], T. YOSHIKAWA[1], Y. TERADA[3], H. NABESHI[1], Y. YOSHIOKA[1,2], N. ITOH[1], Y. TSUTSUMI[1,2]

Received March 25, 2011, accepted May 2, 2011

Tomoaki Yoshikawa, Ph.D., Yasuo Tsutsumi, Ph.D., Department of Toxicology and Safety Science, Graduate School of Pharmaceutical Sciences, Osaka University, 1-6 Yamadaoka, Suita, Osaka 565-0871, Japan.
tomoaki@phs.osaka-u.ac.jp, ytsutsumi@phs.osaka-u.ac.jp
**Both authors contributed equally to the work.*

Pharmazie 65: 808–809 (2011)
doi: 10.1691/ph.2011.1041

Recent studies into the *in vivo* absorption and biological influence of particulate matter, especially nanomaterials (NMs), have raised worldwide concerns over their safety. However, it is often technically difficult to conduct these studies because NMs are too small to be observed by optical microscopy. Here, we attempted to establish a new method to visually detect NMs on tissue samples. Specifically, we have analyzed titanium dioxide particles with a diameter of 5 μm, which are widely used in cosmetics, using frozen tissue sections by synchrotron radiation X-ray fluorescence analysis.

With the recent development of the nanotechnology, nanomaterials (NMs) have been successfully employed in various industrial applications such as medicine, cosmetics, and food (Kaur et al. 2007; Cormode et al. 2010). NMs display a number of useful properties, such as high levels of electrical conductivity, tensile strength, electronic reactivity and tissue permeability, which are not evident in bulk materials (Rutherglen et al. 2009). However, recent studies suggest that NMs may pose a serious risk to human health, which differs from the toxicity of bulk materials (Nel et al. 2006; Shvedova et al. 2010). For assessing the safety of NMs, it is very important to identify their location within the body. In particular, NMs show unique dynamics that allow them to penetrate biological barriers (Nabeshi et al. 2011). Microscopic studies using transmission electron microscopic (TEM) analysis have been used by various researchers (Jin et al. 2008; Chen et al. 2010; Zhang et al. 2010). Many research groups are attempting to develop imaging techniques that will facilitate the visual detection of NMs in tissue samples. Such an approach is expected to greatly assist in the assessment of the biological effects of NMs.

Here, we describe the development of a method to detect titanium dioxide (TiO_2) using frozen sections by synchrotron radiation X-ray fluorescence (SR-XRF) analysis sourced from a synchrotron radiation facility (SPring-8 in Japan). Nanometer sized TiO_2 particles are widely employed in cosmetic products. Here, we used TiO_2 particles with a diameter of 5 μm as a model material for our investigations. Firstly, we observed TiO_2 particles on a frozen section of mouse lung using an optical microscope. We prepared the lung sample by injecting a large dose of TiO_2 into the tail vein of mice. As expected, the agglomerates of TiO_2 particles were observed as black areas (Fig. A). Subsequently, we conducted SR-XRF on the same section in order to verify that SR-XRF could detect titanium (Ti) at the corresponding location (see photomicrograph in Fig. B). These results indicate that SR-XRF is useful for detecting TiO_2 particles in frozen tissue sections.

SR-XRF-mediated detection of TiO_2 particles is a novel technique that has several advantages as described below. Firstly, our method is highly versatile given that SR-XRF can more readily detect elements as their atomic number increase. Thus, NMs such as nano-platinum, nano-silver and nano-zinc oxide will be easily detected by this method. Furthermore, our technique facilitates a direct correspondence between the localization of NMs in the tissue and pathological findings in the tissue samples. However, unlike TEM analysis, our method cannot observe the actual appearance of single NMs in the tissue sample. Moreover, unlike inductively coupled plasma mass spectrometry (ICP-MS), our method cannot quantify the amount of NMs in the tissue sample. It must be emphasized that this study examined the utility of SR-XRF for the detection of particulate matter on frozen tissue sections using only micro-TiO_2 particles. Therefore, further studies using nano-TiO_2 are required. Nonetheless our new method, in conjunction with established complementarily approaches such as TEM or ICP-MS, is expected to provide valuable information concerning the safety of NMs.

In conclusion, we present a new method for detecting and localizing nano-TiO_2 in frozen tissue sections. Although further investigations are needed, we believe our novel technique will complement conventional methodologies to help assess the biological effects of NMs.

Experimental

1. TiO_2 particles

Rutile TiO_2 with a diameter less than 5 μm was purchased from Sigma-Aldrich (St. Louis, MO, USA). The TiO_2 particles were dissolved in solvents and subsequently sonicated for 10 min and vortexed for 1 min prior to use.

2. Animals

Female BALB/c mice were purchased from SLC, Inc (Shizuoka, Japan) and used at 7 weeks of age. All of the animal experimental procedures used in this study were performed in accordance with the National Institute of Biomedical Innovation guidelines for the welfare of animals.

3. Preparation of tissue samples

For the detection of TiO_2 in lung, BALB/c mice were treated with 2 mg/mouse TiO_2 in PBS *via* intravenous injection into the tail. Several minutes after injection of TiO_2 the lung sample was collected. Lung samples were frozen in O.C.T. Compound (Sakura Finetek Japan, Tokyo, Japan) by liquid nitrogen and cut into 20 μm thick sections using a cryomicrotome (Leica Microsystems Japan, Tokyo, Japan) and laid on a Kapton® film.

4. SR-XRF

Tissue sections were observed by optical microscopy. Images were captured in order to determine the area under investigation. Subsequently, SR-XRF was performed using precisely the same area of tissue section. Experiments were carried out at BL37XU of SPring-8, Hyogo, Japan (Terada et al. 2004). The sections were subjected to two-dimensional SR-XRF. The incident beam was monochromatized with a Si (111) double-crystal monochromator to an energy of 10 keV. The monochromatized beam was focused by total-reflection mirrors with Kirkpatrick–Baez configuration into a 0.9 (horizontal) × 1.1 (vertical)-μm^2 microbeam at the sample position. The samples were set on the XY stage and irradiated with this beam. The fluorescence X-rays of the Ti-Kα lines generated from the samples were

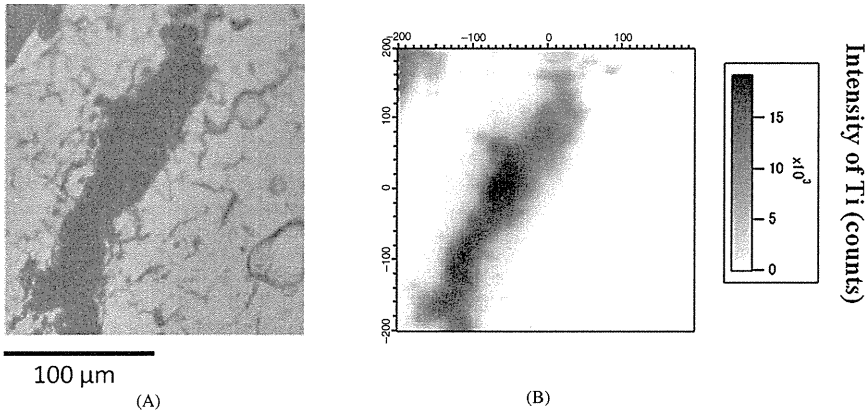

Fig.: Optical microscope image and the 2D-image of Ti distributions in the frozen section of lung. BALB/c mice were treated with 2 mg/mouse TiO_2 in PBS *via* intravenous injection. After sacrificing the mice, lung samples were collected and observed by optical microscopy (A) and SR-XRF (B). The imaging area was 40000 μm^2. Black areas observed in the microscopic image correspond to Ti.

measured by a silicon drift detector positioned perpendicular to the incident X-ray beam. The 2D-imagings of Ti distributions in the samples were obtained by scanning the sample stage along the x-y axes during fluorescent X-ray detections. The measurement time was 0.1 s/step. The scanning range was tuned to 200 μm^2 with 2 μm steps. The images were stored as digital data. These data were restored to images by IGOR Pro (WaveMetrics, OR).

Acknowledgements: This study was supported in part by Grants-in-Aid for Scientific Research from the Ministry of Education, Culture, Sports, Science and Technology of Japan, and from the Japan Society for the Promotion of Science (JSPS). This study was also supported in part by Health Labour Sciences Research Grants from the Ministry of Health, Labor and Welfare of Japan; by Health Sciences Research Grants for Research on Publicly Essential Drugs and Medical Devices from the Japan Health Sciences Foundation; by a Global Environment Research Fund from Minister of the Environment; and by a the Knowledge Cluster Initiative; and by Food Safety Commission; and by The Nagai Foundation Tokyo; and by The Cosmetology Research Foundation; and by The Smoking Research Foundation; and by The Takeda Science Foundation. The synchrotron radiation experiments were performed under the approval of SPring-8 Proposal Review Committee (Proposal No. 2009B1036).

References

Chen YS, Hung YC, Lin LW, Liau I, Hong MY, Huang GS (2010) Size-dependent impairment of cognition in mice caused by the injection of gold nanoparticles. Nanotechnology 21: 485102.

Cormode DP, Jarzyna PA, Mulder WJ, Fayad ZA (2010) Modified natural nanoparticles as contrast agents for medical imaging. Adv Drug Delivery Rev 62: 329–338.

Jin CY, Zhu BS, Wang XF, Lu QH (2008) Cytotoxicity of titanium dioxide nanoparticles in mouse fibroblast cells. Chem Res Toxicol 21: 1871–1877.

Nabeshi H, Yoshikawa T, Matsuyama K, Nakazato Y, Matsuo K, Arimori A, Isobe M, Tochigi S, Kondoh S, Hirai T, Akase T, Yamashita T, Yamashita K, Yoshida T, Nagano K, Abe Y, Yoshioka Y, Kamada H, Imazawa T, Itoh N, Nakagawa S, Mayumi T, Tsunoda T, Tsutsumi Y (2011) Systemic distribution, nuclear entry and cytotoxicity of amorphous nanosilica following topical application. Biomaterials 32: 2713–2724.

Kaur IP, Agrawal R (2007) Nanotechnology: a new paradigm in cosmeceuticals. Recent Pat Drug Delivery Formulation 1: 171–182.

Nel A, Xia T, Madler L, Li N (2006) Toxic potential of materials at the nanolevel. Science 311: 622–627.

Rutherglen C, Burke P (2009) Nanoelectromagnetics: circuit and electromagnetic properties of carbon nanotubes. Small 5: 884–906.

Shvedova AA, Kagan VE, Fadeel B (2010) Close encounters of the small kind: adverse effects of man-made materials interfacing with the nano-cosmos of biological systems. Annu Rev Pharmacol Toxicol 50: 63–88.

Terada Y, Goto S, Takimoto N, Takeshita K, Yamazaki H, Shimizu Y, Takahashi S, Ohashi H, Furukawa Y, Matsushita T, Ohata T, Ishizawa Y, Uruga T, Kitamura H, Ishikawa T, Hayakawa S (2004) Construction and Commissioning of BL37XU at SPring-8. AIP Conf Proc 705: 376–379.

Zhang Q, Hitchins VM, Schrand AM, Hussain SM, Goering PL (2010) Uptake of gold nanoparticles in murine macrophage cells without cytotoxicity or production of pro-inflammatory mediators. Nanotoxicology 0: 1–12.

Laboratory of Bio-Functional Molecular Chemistry[1] and Laboratory of Toxicology and Safety Science[2], Graduate School of Pharmaceutical Sciences, Osaka University; Laboratory of Biopharmaceutical Research (Pharmaceutical Proteomics)[3], National Institute of Biomedical Innovation, Osaka, Japan

Hepatotoxicity of silica nanoparticles with a diameter of 100 nm

T. HASEZAKI[1], K. ISODA[1], M. KONDOH[1], Y. TSUTSUMI[2,3], K. YAGI[1]

Received February 1, 2011, accepted February 25, 2011

Dr. Kiyohito Yagi, Laboratory of Bio-Functional Molecular Chemistry, Graduate School of Pharmaceutical Sciences, Osaka University, Suita, Osaka 565-0871, Japan
yagi@phs.osaka-u.ac.jp

Pharmazie 66: 698–703 (2011) *doi: 10.1691/ph.2011.1516*

Nanomaterials have potential toxicity that is not found in micromaterials, and it is therefore essential to understand their biological activity and potential toxicity. We focused on silica nanoparticles, since it was previously reported that the intravenous administration of silica nanoparticles with a diameter of 70 nm (SP70) causes hepatic injury. In the present study, we focused on the effects of the particle diameter of silica. We found that silica nanoparticles caused acute liver toxicity at a diameter of 100 nm, and that liver sinusoidal endothelial cells are directly involved in silica nanoparticle-induced liver injury. These findings suggest that the diameter of nanoparticles has great influence on silica nanoparticle-induced liver injury.

1. Introduction

Nanoparticles are generally defined as having diameters of 100 nm or less (Stone et al. 2007; Tsuda et al. 2009). Nanomaterials are used frequently in microelectronics, cosmetics, and semiconductor materials, and research for the development of nanomaterial-based drug delivery systems is promising. As such, there has been a tendency to decrease the grain diameter from the micro to the nano scale in a variety of industrial fields. However, nanosized particles have a potential for toxicity that does not exist for microparticles. It is therefore imperative to understand the biological activity and potential toxicity of nanosized particles (Bystrzejewska-Piotrowska et al. 2009; Warheit et al. 2008).

Silica is the oxide of silicon, and has a large, porous outer structure with a variety of useful characteristics (Kobler and Bein 2008). Silica is commonly used as an industrial material due to its durability and general applicability (Mc Nally et al. 2006). It has been reported that non-crystalloid silica particles at the micrometer scale are completely safe for human exposure (Martin 2007). However, silica nanoparticles are increasingly used as materials in the electronics industry because they serve as a unique substrate (Chung et al. 2009). It is thought that the production of silica nanoparticles will be expanded in the future; however, little is known about their toxicity.

Since nanoparticles are a unique substrate, it follows that their effects on the living body are also unique, and therefore potentially problematic. It is thought that the size and surface area of the particles are important factors in their influence on the living body (Merget et al. 2002). Therefore, decreasing the size of the particles increases their potential influence on living things.

Abbreviations: SP70 70 nm silica particles; SP100 100 nm silica particles; SP300 300 nm silica particles; CDDP cisplatin; PQ paraquat; ALT alanine aminotransferase; AST aspartate aminotransferase; BUN blood urea nitrogen.

We previously reported that silica nanoparticles with a diameter of 70 nm cause liver injury, whereas silica nanoparticles of a diameter of 300 nm do not (Nishimori et al. 2009a, c). This implies that the hepatic toxicity of silica nanoparticles has a specific threshold determined by the grain diameter. In this study, to examine the effects of silica nanoparticles in liver injury, silica nanoparticles of a diameter of 100 nm were used. In addition, we examined the mechanism by which silica nanoparticles caused liver injury, and investigated the synergistic effects on hepatic toxicity of SP100 with pharmaceutical agents.

2. Investigations, results and discussion

2.1. Acute toxicity of 100-nm-diameter silica nanoparticles

We initially examined liver injury caused by silica nanoparticles with diameters of 100 nm (SP100), and investigated the acute liver toxicity of silica nanoparticles with diameters of 100 nm at a maximal dose of 100 mg/kg (Fig. 1). Acute liver toxicity of SP100 rose dose-dependently (Fig. 1A). Intravenous injection of SP100 at 100 mg/kg was often lethal in mice. There was acute liver toxicity of SP100 at 60 mg/kg. Moreover, elevation of blood urea nitrogen, a biochemical marker of kidney injury, was not observed (Fig. 1B). These data demonstrated that silica nanoparticles caused acute liver toxicity at a diameter of 100 nm. Next, SP100 at doses of 60 mg/kg, SP70 at 40 mg/kg, and SP300 at 100 mg/kg were administered to mice. As shown in Fig. 2A, at 24 h after silica nanoparticle treatment, the levels of serum ALT after SP70 treatment greatly increased. There was no liver injury caused by SP300, though there was liver injury caused by SP100. Figure 2 (B-E) shows hematoxylin-eosin staining of the liver in silica nanoparticle-injected mice. Liver injury was confirmed in SP70 and SP100 treated mice, but not in SP300 treated mice. These results show that silica nanoparticles with a diameter of 100 nm and below cause liver toxicity.

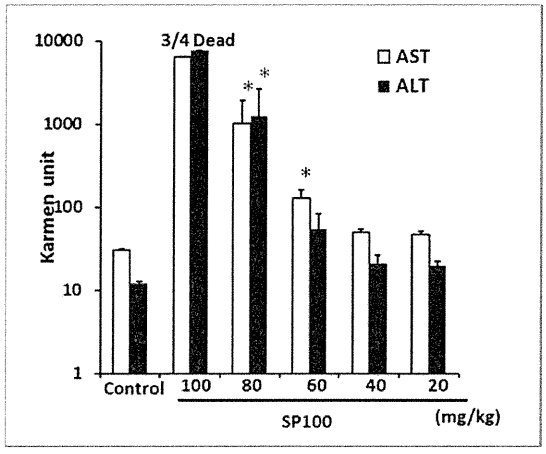

(A)

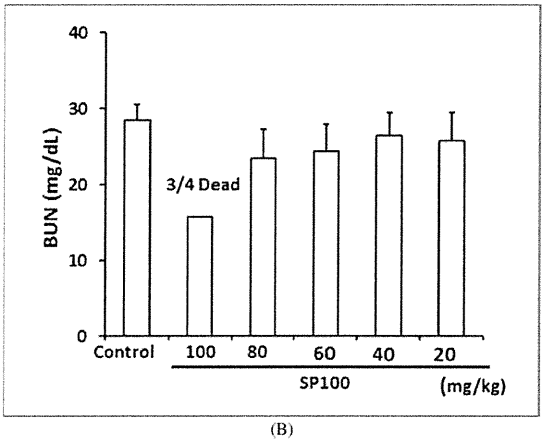

(B)

Fig. 1: Dose-dependency of SP100 on liver and kidney injury SP100 was intravenously administered at the indicated doses. Serum ALT, AST, (A) and BUN (B) at 24 h were measured using a commercially available kit, as described in the Experimental section. Data are means ± SEM (n = 4). *Significantly different compared with the vehicle-treated group ($p < 0.05$).

Nanosized particles are defined as having a grain diameter of 100 nm or less. Our results showed that there was hepatic toxicity caused by SP100 and SP70, but not by SP300. Vamanu et al. (2008) reported that TiO_2 nanoparticles of a diameter of 100 nm or less are cytotoxic. Additionally, Shavandi et al. (2010) reported that silver nanoparticles of a diameter of 100 nm or less are cytotoxic. These results show that the grain diameter is critical for determining the level of toxicity to the body and to cells, and in particular, they imply that toxicity is induced by particles of 100 nm or less.

The acute liver toxicity of SP100 increased in a dose-dependent manner (Figs. 1, 2). Moreover, we assessed the presence of liver fibrosis in SP100 treatments. SP100 significantly increased the hepatic hydroxyproline content (data not shown). We previously found that SP70 causes acute liver toxicity and hepatic fibrosis (Nishimori et al. 2009a, c). In the present study, we found that SP70 had a larger effect on liver damage compared to SP100 (Fig. 2). These results show that the level of hepatic toxicity changes according to the grain diameter of the silica particles. In future studies, it will be necessary to examine the level of hepatic toxicity caused by a wide variety of grain diameters of silica nanoparticles.

2.2. Mechanism of acute liver toxicity by silica nanoparticles

We investigated the liver toxicity caused by silica nanoparticles when combined with agents that inhibit the activities of liver sinusoidal endothelial cells or liver Kupffer cells. Cyclophosphamide (CPA) is an alkylating agent that induces apoptosis in liver sinusoidal endothelial cells (DeLeve 1996; Malhi et al. 2002). $GdCl_3$ inhibits phagocytosis by Kupffer cells and transiently eliminates them, and $GdCl_3$ has been widely used to investigate the roles of Kupffer cells in the liver (Hardonk et al. 1992; van Til et al. 2005). We thus investigated the effects of CPA and $GdCl_3$ on silica nanoparticle-induced liver injury. As shown in Fig. 3A, pre-injection of CPA did not affect the ALT levels in mice, whereas in silica nanoparticle-injected mice, CPA dramatically decreased ALT levels to near control values. Moreover, as shown in Fig. 3B, pre-injection of $GdCl_3$ prior to injection of silica nanoparticles elevated serum ALT levels 2-fold or more in the silica nanoparticle-injected group. Next, we investigated the cytotoxicity of SP70, SP100, and SP300 in primary cultured hepatocytes isolated from mice. SP70 and SP100 at 100 μg/ml were toxic to primary hepatocytes to almost the same degree, indicating that the differences in liver injury among these nanoparticles were not due to differences in the sensitivity of hepatocytes to the nanoparticles (Fig. 3C). These data indicated that liver sinusoidal endothelial cells are directly involved in silica nanoparticle-induced liver injury, and that phagocytosis of silica nanoparticles by Kupffer cells attenuates liver injury.

Liver sinusoidal endothelial cells form the basic tubular vessels for transvascular exchange between the blood and the surrounding tissue (McCuskey 2008). Kupffer cells are a component of the sinusoidal wall and play a significant role in the removal of particles and cells as well as toxic substances (Wisse et al. 1996). We observed that the ALT values decreased to near control levels by the administration of silica nanoparticles and CPA (Fig. 3A). This indicates that liver sinusoidal endothelial cells greatly influence the hepatic toxicity by silica nanoparticles. There are several receptors on the cell surface of liver sinusoidal endothelial cells, and it is known that they endocytose proteins and large particles (Smedsrod et al. 1997; Steffan et al. 1986). It is likely that silica nanoparticles are englobed by liver sinusoidal endothelial cells, after which they accumulate and are then discharged into hepatocytes. A detailed analysis of the relationship between liver sinusoidal endothelial cells and silica nanoparticles is necessary for future studies.

2.3. Influence of 100-nm-diameter silica nanoparticles with cisplatin or paraquat-induced toxicity

Previously, we reported synergistic toxicity of SP70 with CDDP and PQ (Nishimori et al. 2009b). CDDP is widely used as an anti-tumor agent, and PQ is one of the most widely used and highly toxic herbicides (Ozols and Young 1991; Vandenbogaerde et al. 1984; Witjes 1997). In the present study, we thus investigated the synergistic effects of hepatic toxicity of SP100 with CDDP or PQ. To avoid direct interactions between the chemicals and SP100 before administration and absorption, we injected the chemicals and SP100 intraperitoneally and intravenously, respectively. We observed that the serum levels of ALT were elevated by CDDP (Fig. 4A). We next investigated the interaction between PQ and SP100. Co-administration of PQ and SP100 elevated levels of serum ALT, and SP100 showed synergistic elevation of serum ALT levels from 138.2 to 492.0 KU (Fig. 4B).

We investigated the combined effects of the chemicals on nanoparticle-induced toxicity, and found that CDDP and PQ had synergistic toxic effects with SP100. Verma et al. reported

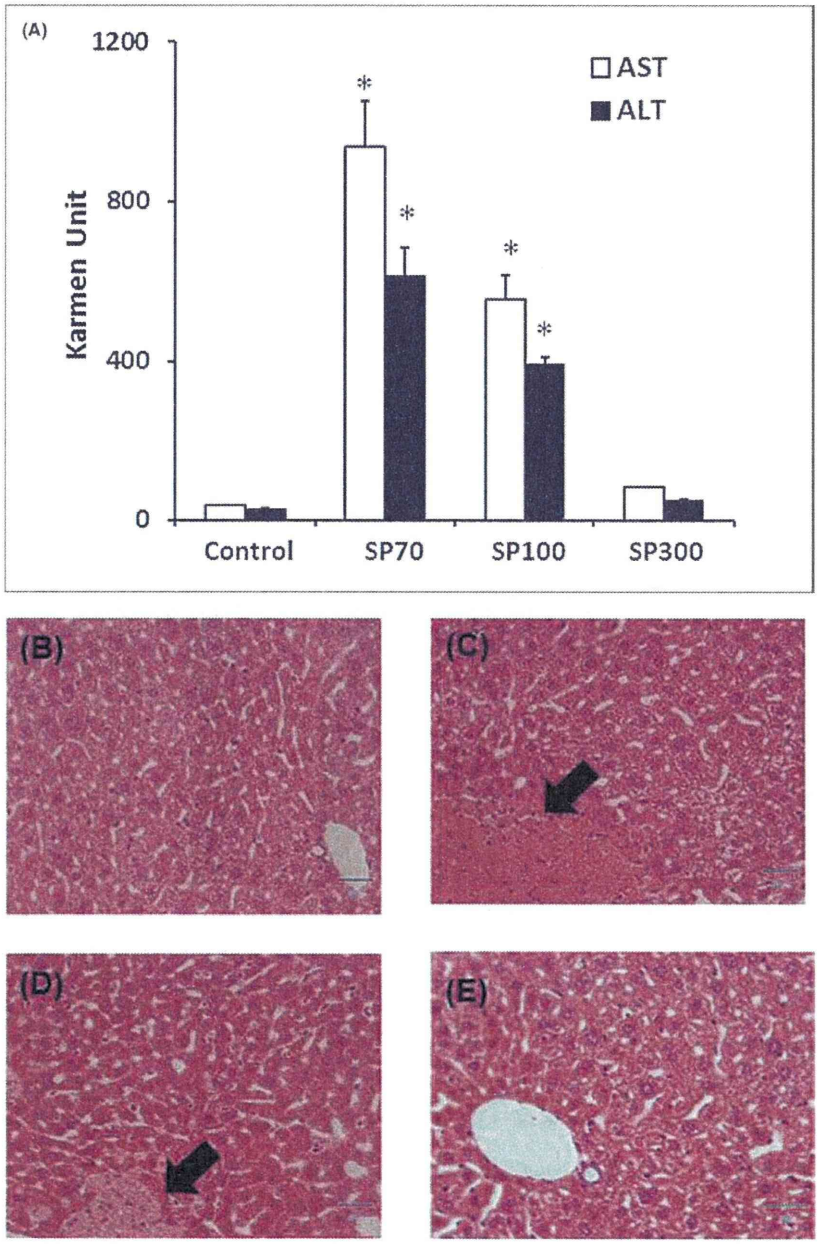

Fig. 2: Comparison of acute liver toxicity of silica nanoparticles Serum ALT and AST (A) at 24 h were measured using a commercially available kit as described in the Experimental section. Histological analysis of silica nanoparticle-treated mice were conduced on tissues fixed with 4% paraformaldehyde 24 h after administration of vehicle (B), SP70 (C), SP100 (D), and SP300 (E). Tissue sections were stained with hematoxylin and eosin and observed under a microscope. Data are representative of at least four mice. Blood was recovered at 24 h after injection. The arrow shows hepatic injury. Data are means ± SEM (n = 4). *Significantly difference compared with the vehicle-treated group ($p < 0.05$).

that the blood circulation levels of CDDP are made to rise by nanomaterial conjugates of CDDP (Verma and Saching 2008). In addition, Moreno et al. (2009) reported that PLGA nanoparticles improve the effects of CDDP. Therefore, nanoparticles could possibly increase both the beneficial effects and toxicity of chemicals and drugs. Further evaluation of such interactions between nanomaterials and pharmaceutical agents for future pharmaceutical applications are necessary.

This report is the first to show that silica nanoparticles with a diameter of 100 nm or less have hepatic toxicity, and that liver injury is mediated by liver sinusoidal endothelial cells. Further studies based on these data should provide useful information regarding the safety of nanomaterials.

3. Experimental

3.1. Materials

Silica particles with a diameter of 70, 100, or 300 nm (SP70, SP100, SP300) were obtained from Micromod Partikeltechnologie GmbH (Rostock,

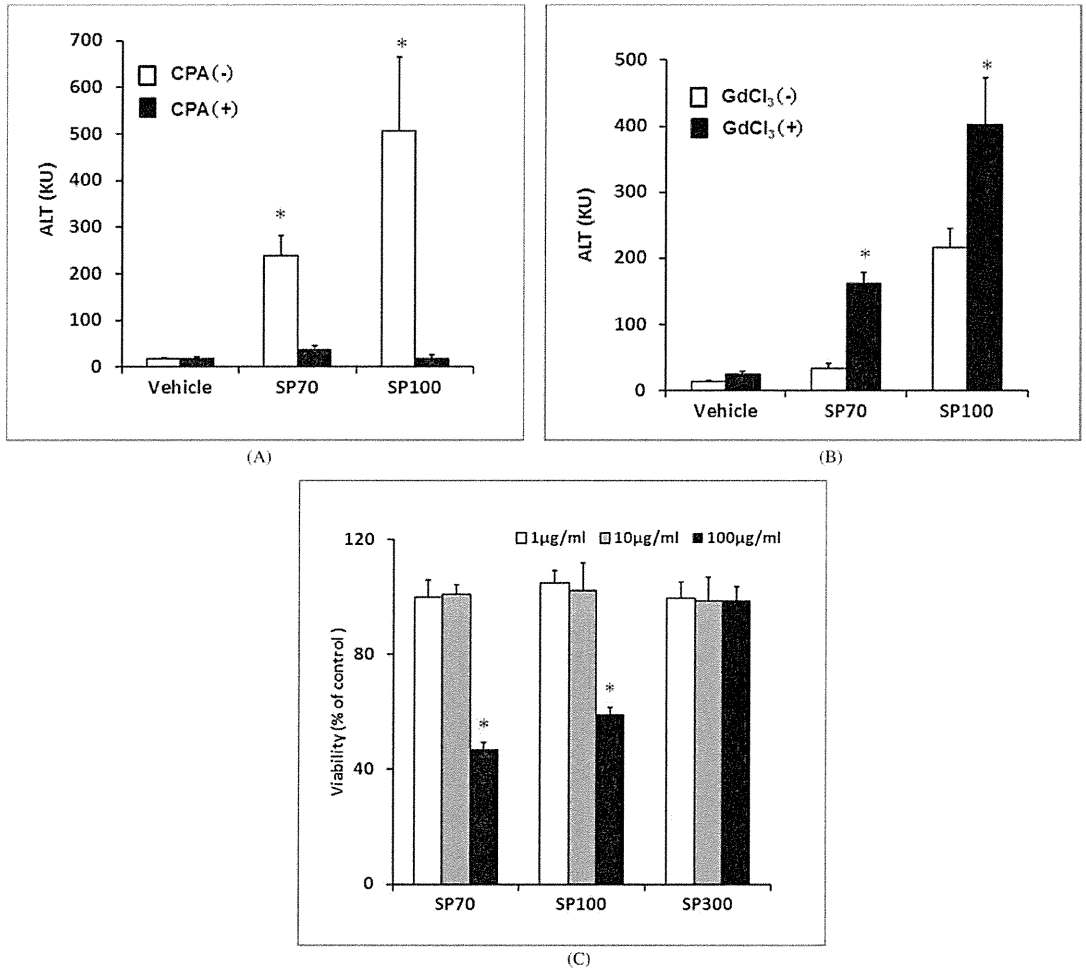

Fig. 3: Analysis of silica nanoparticle-induced liver injury Effect of CPA (A). Vehicle or CPA (300 mg/kg) was intraperitoneally injected into mice 24 h prior to treatment with silica particles (SP70, 40 mg/kg; SP100, 60 mg/kg). At 24 h after administration of particles, blood was recovered, and the resultant serum was used for ALT assay. Data are means ± SEM (n = 4). *Significant difference between vehicle and silica particle-treated groups ($p < 0.05$). Effect of $GdCl_3$ (B). Vehicle or $GdCl_3$ (10 mg/kg) was intravenously injected into mice at 30 h or 6 h prior to treatment with silica particles. 24 h after particle administration, blood was recovered, and the resultant serum was used for ALT assay. Data are means ± SEM (n = 4). *Significant difference between $GdCl_3$ + and $GdCl_3$ - groups ($p < 0.05$). (C) Comparison of cytotoxicity of silica nanoparticles in primary hepatocytes. Hepatocytes were prepared from mouse livers by the collagenase perfusion method, as described in the Experimental section. Cells were seeded onto 96-well plates at 5×10^3 cells/well, and were treated with silica particles at the indicated concentrations. After 48 h of treatment, viability was measured by WST-8 assay as described in the Materials and methods. Data were normalized against vehicle-treated cells (100% control). Data are means ± SD (n = 4).

Germany). The size distribution of the particles was analyzed using a Zetasizer (Sysmex Co., Kobe, Japan), and the mean diameters were 57.5 ± 20.3, 137 ± 32.1, and 296 ± 36.3 nm, respectively. The particles were spherical and nonporous and were stored at 25 or 50 mg/mL in an aqueous suspension. The suspensions were thoroughly dispersed with sonication before use and then diluted in ultrapure water. Paraquat (PQ) and cisplatin (CDDP) were dissolved in saline and stored at −20 °C before use. All reagents used were of research grade.

3.2. *Animals*

Eight-week-old BALB/c male mice were purchased from Shimizu Laboratory Supplies Co., Ltd. (Kyoto, Japan) and were maintained in a controlled environment (23 ± 1.5 °C; 12-h light/dark cycle) with access to standard rodent chow and water *ad libitum*. The mice were left to adapt to the new environment for 1 week before commencing with the experiment. Mice that received a single treatment of silica nanoparticles were anesthetized and sacrificed 24 h after intravenous injection. The experimental protocols conformed to the ethical guidelines of the Graduate School of Pharmaceutical Sciences, Osaka University.

3.3. *Biochemical analysis*

Serum alanine aminotransferase (ALT) and blood urea nitrogen (BUN) were measured with commercially available kits according to the manufacturer's protocols (Wako Pure Chemical Industries, Osaka, Japan).

3.4. *Histological analysis*

The liver was removed and fixed with 4% paraformaldehyde. After sectioning, thin tissue sections were stained with hematoxylin and eosin for histological observation.

3.5. *Cyclophosphamide assay*

Disruption of liver sinusoidal endothelial cells was carried out by intraperitoneal injection of 300 mg/kg body weight cyclophosphamide (CPA) at 24 h prior to administration of nanoparticles. Blood was recovered at 24 h after injection of nanoparticles for the ALT assay.

3.6. *Gadolinium chloride assay*

For Kupffer cell blockage of phagocytosis and partial depletion in the liver, mice were injected intravenously with gadolinium chloride ($GdCl_3$) at

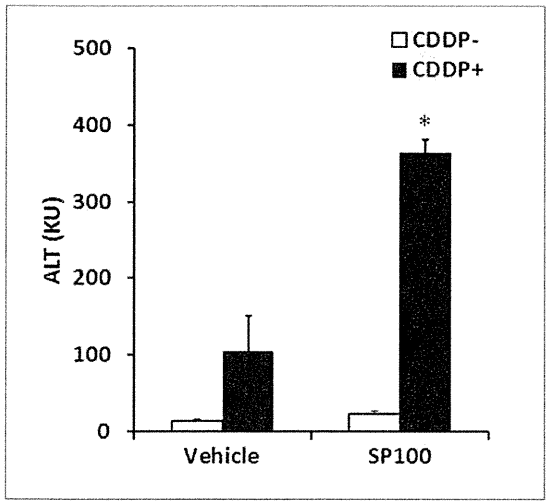

(A)

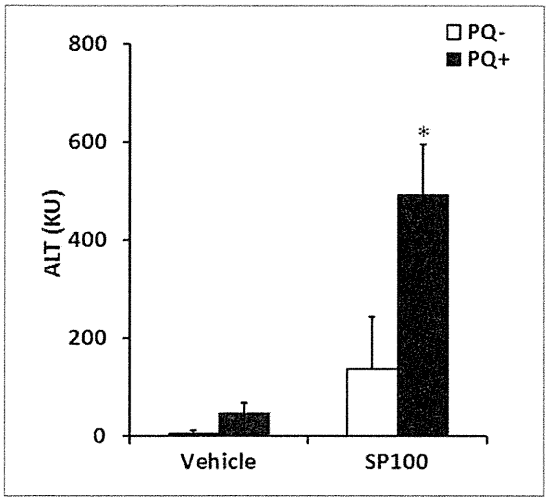

(B)

Fig. 4: Effect of SP100 on cisplatin- and paraquat-induced toxicity (A) Mice were injected with cisplatin (CDDP) at 0 or 50 μmol/kg and SP100 at 10 mg/kg, intraperitoneally and intravenously, respectively. At 24 h post-injection, the serum was recovered. ALT levels were assayed as described in the Experimental section. Data are means ± SEM (n = 4). *Significant difference between vehicle and CDDP-treated group ($p < 0.05$). (B) Mice were injected with paraquat (PQ) at 0 or 50 mg/kg and SP100 at 60 mg/kg, intraperitoneally and intravenously, respectively. At 24 h post-injection, the serum was recovered. ALT levels were assayed as described in the experimental section. Data are means ± SEM (n = 4). *Significant difference between vehicle and PQ-treated group ($p < 0.05$).

10 mg/kg body weight at 30 h and 6 h prior to intravenous administration of nanoparticles. Blood was then recovered 24 h after injection of nanoparticles for the ALT assay.

3.7. Cytotoxicity in primary hepatocytes

Hepatocytes were isolated from BALB/c mice by Seglen's method using perfusion of collagenase (Seglen 1976). Viability of the isolated hepatocytes was assayed by trypan blue staining, and cells (over 90% viability) were seeded onto 96-well plates at 5×10^3 cells/well, and the cells were treated with silica particles for 48 h. Cell viability was then assayed with the Cell Counting Reagent SF, according to the manufacturer's protocol (Nacalai Tesque, Kyoto Japan).

References

Bystrzejewska-Piotrowska G., Golimowski J, Urban PL (2009) Nanoparticles: their potential toxicity, waste and environmental management. Waste Manag 29: 2587–2595.

Chung EA, Koo J, Lee M, Jeong DY, Kim S (2009) Enhancement-mode silicon nanowire field-effect transistors on plastic substrates. Small 5: 1821–1824.

DeLeve LD (1996) Cellular target of cyclophosphamide toxicity in the murine liver: role of glutathione and site of metabolic activation. Hepatology 24: 830–837.

Hardonk MJ, Dijkhuis FW, Hulstaert CE, Koudstaal J (1992) Heterogeneity of rat liver and spleen macrophages in gadolinium chloride-induced elimination and repopulation. J Leukoc Biol 52: 296–302.

Kobler J, Bein T (2008) Porous thin films of functionalized mesoporous silica nanoparticles. ACS Nano 2: 2324–2330.

Malhi H, Annamaneni P, Slehria S, Joseph B, Bhargava KK, Palestro CJ, Novikoff PM, Gupta S (2002) Cyclophosphamide disrupts hepatic sinusoidal endothelium and improves transplanted cell engraftment in rat liver. Hepatology 36: 112–121.

Martin, KR (2007) The chemistry of silica and its potential health benefits. J Nutr Health Aging 11: 94–97.

Mc Nally L, O'Sullivan DJ, Jagger DC (2006) An *in vitro* investigation of the effect of the addition of untreated and surface treated silica on the transverse and impact strength of poly(methyl methacrylate) acrylic resin. Biomed Mater Eng 16: 93–100.

McCuskey RS (2008) The hepatic microvascular system in health and its response to toxicants. Anat Rec (Hoboken) 291: 661–671.

Merget R, Bauer T, Kupper HU, Philippou S, Bauer HD, Breitstadt R, Bruening T (2002) Health hazards due to the inhalation of amorphous silica. Arch Toxicol 75: 625–634.

Moreno D, Zalba S, Navarro I, Tros de Ilarduya C, Garrido MJ (2009) Pharmacodynamics of cisplatin-loaded PLGA nanoparticles administered to tumor-bearing mice. Eur J Pharm Biopharm 74: 265–274.

Nishimori H, Kondoh M, Isoda K, Tsunoda S, Tsutsumi Y, Yagi K (2009a) Histological analysis of 70-nm silica particles-induced chronic toxicity in mice. Eur J Pharm Biopharm 72: 626–629.

Nishimori H, Kondoh M, Isoda K, Tsunoda S, Tsutsumi Y, Yagi K (2009b) Influence of 70 nm silica particles in mice with cisplatin or paraquat-induced toxicity. Pharmazie 64: 395–397.

Nishimori H, Kondoh M, Isoda K, Tsunoda S, Tsutsumi Y, Yagi K (2009c) Silica nanoparticles as hepatotoxicants. Eur J Pharm Biopharm 72: 496–501.

Ozols RF, Young RC (1991) Chemotherapy of ovarian cancer. Semin Oncol 18: 222–232.

Seglen PO (1976) Preparation of isolated rat liver cells. Methods Cell Biol 13: 29–83.

Shavandi Z, Ghazanfari T, Moghaddam KN (2010) *In vitro* toxicity of silver nanoparticles on murine peritoneal macrophages. Immunopharmacol Immunotoxicol. 27.

Smedsrod B, Melkko J, Araki N, Sano H, Horiuchi S (1997) Advanced glycation end products are eliminated by scavenger-receptor-mediated endocytosis in hepatic sinusoidal Kupffer and endothelial cells. Biochem J 322 (Pt 2): 567–573.

Steffan AM, Gendrault JL, McCuskey RS, McCuskey PA, Kirn A (1986) Phagocytosis, an unrecognized property of murine endothelial liver cells. Hepatology 6: 830–836.

Stone V, Johnston H, Clift MJ (2007) Air pollution, ultrafine and nanoparticle toxicology: cellular and molecular interactions. IEEE Trans Nanobioscience 6: 331–340.

Tsuda H, Xu J, Sakai Y, Futakuchi M, Fukamachi K (2009) Toxicology of engineered nanomaterials - a review of carcinogenic potential. Asian Pac J Cancer Prev 10: 975–980.

Vamanu CI, Cimpan MR, Hol PJ, Sornes S, Lie SA, Gjerdet NR (2008) Induction of cell death by TiO_2 nanoparticles: studies on a human monoblastoid cell line. Toxicol *In Vitro* 22: 1689–1696.

van Til NP, Markusic DM, van der Rijt R, Kunne C, Hiralall JK, Vreeling H, Frederiks WM, Oude-Elferink RP, Seppen J (2005) Kupffer cells and not liver sinusoidal endothelial cells prevent lentiviral transduction of hepatocytes. Mol Ther 11: 26–34.

Vandenbogaerde J, Schelstraete J, Colardyn F, Heyndrickx A (1984) Paraquat poisoning. Forensic Sci Int 26: 103–114.

Verma AK, Sachin K (2008) Novel hydrophilic drug polymer nanoconjugates of Cisplatin showing long blood retention profile: its release

kinetics, cellular uptake and bio-distribution. Curr Drug Deliv 5: 120–126.

Warheit DB, Sayes CM, Reed KL, Swain KA (2008) Health effects related to nanoparticle exposures: environmental, health and safety considerations for assessing hazards and risks. Pharmacol Ther 120: 35–42.

Wisse E, Braet F, Luo D, De Zanger R, Jans D, Crabbe E, Vermoesen A (1996) Structure and function of sinusoidal lining cells in the liver. Toxicol Pathol 24: 100–111.

Witjes JA (1997) Current recommendations for the management of bladder cancer. Drug therapy. Drugs 53: 404–414.

Hirai et al. Particle and Fibre Toxicology 2012, 9:3
http://www.particleandfibretoxicology.com/content/9/1/3

PARTICLE AND FIBRE TOXICOLOGY

RESEARCH Open Access

Amorphous silica nanoparticles size-dependently aggravate atopic dermatitis-like skin lesions following an intradermal injection

Toshiro Hirai[1,2], Tomoaki Yoshikawa[1,2*], Hiromi Nabeshi[1,2], Tokuyuki Yoshida[1,2], Saeko Tochigi[1,2], Ko-ichi Ichihashi[1,2], Miyuki Uji[1,2], Takanori Akase[1,2], Kazuya Nagano[2], Yasuhiro Abe[2], Haruhiko Kamada[2,3], Norio Itoh[1,2], Shin-ichi Tsunoda[2,3], Yasuo Yoshioka[2,3] and Yasuo Tsutsumi[1,2,3*]

Abstract

Background: Due to the rising use of nanomaterials (NMs), there is concern that NMs induce undesirable biological effects because of their unique physicochemical properties. Recently, we reported that amorphous silica nanoparticles (nSPs), which are one of the most widely used NMs, can penetrate the skin barrier and induce various biological effects, including an immune-modulating effect. Thus, it should be clarified whether nSPs can be a risk factor for the aggravation of skin immune diseases. Thus, in this study, we investigated the relationship between the size of SPs and adjuvant activity using a model for atopic dermatitis.

Results: We investigated the effects of nSPs on the AD induced by intradermaly injected-mite antigen *Dermatophagoides pteronyssinus* (Dp) in NC/Nga mice. Ear thickness measurements and histopathological analysis revealed that a combined injection of amorphous silica particles (SPs) and Dp induced aggravation of AD in an SP size-dependent manner compared to that of Dp alone. In particular, aggravation was observed remarkably in nSP-injected groups. Furthermore, these effects were correlated with the excessive induction of total IgE and a stronger systemic Th2 response. We demonstrated that these results are associated with the induction of IL-18 and thymic stromal lymphopoietin (TSLP) in the skin lesions.

Conclusions: A particle size reduction in silica particles enhanced IL-18 and TSLP production, which leads to systemic Th2 response and aggravation of AD-like skin lesions as induced by Dp antigen treatment. We believe that appropriate regulation of nanoparticle physicochemical properties, including sizes, is a critical determinant for the design of safer forms of NMs.

Keywords: Nanoparticle, Silica, Allergy, Cytokines

Background

With the development of nanotechnology, practical uses for nanomaterials (NMs) are rapidly spreading to a wide variety of fields, such as cosmetics, food, and medicine, because they have unique physicochemical properties and exert innovative functions [1-3]. These observations mean that intentional exposure of NMs is unavoidable in everyday life. However, it is a concern that NMs can exhibit unknown harmful effects [4,5]. For example, maternal exposure to titanium dioxide nanoparticles ($nTiO_2$) induces gene expression alterations related to brain development [6]. We also revealed that amorphous silica nanoparticles (nSPs) and $nTiO_2$ induce reproductive and/or liver toxicity compared with submicron-sized amorphous silica particles (SPs) [7,8]. However, little information exists on the potential hazard of NMs. To ensure the safety of NMs and enjoy their many benefits, it is essential to obtain more information on the relationship between the factors associated with NM hazards and their physicochemical properties, such as size and surface properties, to design safer forms of NMs.

* Correspondence: tomoaki@phs.osaka-u.ac.jp; ytsutsumi@phs.osaka-u.ac.jp
[1]Laboratory of Toxicology and Safety Science, Graduate School of Pharmaceutical Sciences, Osaka University, 1-6, Yamadaoka, Suita, Osaka 565-0871, Japan
Full list of author information is available at the end of the article

nSPs are used as a base material in cosmetics and an anti-caking agent in food because of their high transparency and coatability [9,10]. Because nSPs are one of the most widely used NMs, the chances of being exposed to nSPs in our daily life are high. Thus, we must analyze the *in vitro*/*in vivo* biodistribution of nSPs including estimations of whether they can penetrate the biological barrier. Additionally, we need to estimate whether they could be responsible for acute/chronic side effects, thereby facilitating a more accurate risk analysis of nSPs. Under these circumstances, we revealed that nSPs with a diameter of 70 nm (nSP70) can penetrate the skin barrier and enter keratinocytes and Langerhans cells [11]. Our studies further revealed that a dermal application of nSP70 induces apoptosis in dermal cells [11]. In addition, we reported that nSPs have a greater cytotoxic effect on Langerhans cells [12]. Thus it is possible that nSPs may be associated with development of the allergic diseases such as atopic dermatitis (AD). However, the relationship between the size of SPs and its adjuvant activity which can affect aggravation of AD like skin lesion has remained unclear.

In present study, we investigated the effect of nSPs on AD-like skin lesions using *Dermatophagoides pteronyssinus* (Dp), which is the main allergen of AD [13], in NC/Nga mice. We also examined the relationship between the SP size and aggravation of AD.

Results

Physicochemical properties of variously sized SPs

Prior to undertaking this study, we first analyzed the physicochemical properties of SPs (Table 1). SPs remained as stable well-dispersed particles in PBS and not as aggregates. Thus, these particles were ideally suited to evaluate whether their biological effects depended on particle size.

Effects of variously sized SPs on AD-like skin lesions

To evaluate whether variously sized SPs affects AD-like skin lesions induced by Dp, we first measured ear thickness on days 0 and 19. We confirmed that the intradermal injection of Dp enhanced ear thickening as compared to that of PBS (Figure 1A). A combined injection of Dp and the submicron-sized SPs, mSP1000 or nSP300, did not enhance ear thickening compared with that of Dp alone. In contrast, a combined injection of Dp + nSPs (nSP100, nSP70, and nSP30) enhanced ear thickening two- to fivefold compared with that of Dp alone. nSP-treatment showed a marked tendency to cause ear thickening. Thus, nSPs with a diameter ≤100 nm acted specifically to enhance ear thickening in this model.

Next, we performed hematoxylin-eosin and toluidine blue staining using ear sections 24 h after the last intradermal injection (Figure 1B and 1D). Then, several representative symptoms (scab, acanthosis, inflammatory cell infiltration, and scleredema) were scored on the H&E sections (Figure 1C). A Dp injection caused significant inflammatory cell infiltration compared with a PBS injection. In contrast, a combined injection of Dp and variously sized SPs caused more severe inflammatory cell infiltration than that of Dp alone. Although the Dp injection did not cause scabs, acanthosis, or scleredema, the combined injection of Dp and SPs with a diameter ≤300 nm caused acanthosis. Furthermore, a combined injection of Dp and nSPs caused significant scabs and scleredema (Figure 1C). Mast cell infiltrates in the skin were stronger following the combined injection of Dp and nSPs (Figure 1D and 1E). Thus, the injection of Dp and submicron-sized SPs caused only inflammatory cell infiltration and acanthosis compared with that of Dp alone. However, injecting Dp and nSPs caused not only inflammatory cell infiltration and acanthosis but also scabs and scleredema. These findings suggest that injecting nSPs with a diameter ≤100 nm and Dp induced severe AD-like histological changes.

Table 1 Summary of the physicochemical properties of amorphous silica particles (SPs).

	Primary particle size (nm)[a]	Diameter in PBS (nm)	Mean zeta potential (mV)	pH
mSP1000	1000	1136 ± 32.1	-33.2 ± 1.4	7.6
nSP300	300	264 ± 7.2	-25.8 ± 0.7	7.4
nSP100	100	106 ± 0.6	-24.3 ± 0.5	7.4
nSP70	70	76 ± 1.7	-19.5 ± 1.0	7.4
nSP30	30	39 ± 4.2	-14.0 ± 1.3	7.4

Mean particle size and zeta potential in solution of silica particles are expressed as mean ± S.D. (n = 3). [a] Information from technical datasheet of products.

Effects of variously sized SPs on the IgE response

Many reports have shown that the total IgE and allergen-specific IgE level correlate with severity of AD [14,15]. To clarify the nSP-mediated aggravation of AD-like lesions, we first measured total IgE and Dp-specific IgE 24 h after the last intradermal injection (Figure 2). The total IgE in the Dp alone group was higher than that in the PBS group (Figure 2A). Furthermore, the levels of total IgE in the Dp + SP groups were enhanced in an SP size-dependent manner compared with those in the Dp alone group. A regression analysis showed that the particle size reduction was a significant contributor to this effect (Figure 2B; $R^2 = 0.98$). Therefore, it paralleled the severity of the AD-like skin lesions. In the presence of variously sized SPs, the Dp-specific IgE levels were significantly increased compared with Dp alone group (Figure 2C). However, Dp-specific IgE levels